Available online at www.sciencedirect.com
ScienceDirect
Journal of the European Ceramic Society 30 (2010) 53–60
www.elsevier.com/locate/jeurceramsoc

Highly porous ZrO_2 ceramics fabricated by a camphene-based freeze-casting route: Microstructure and properties

Jiecai Han, Changqing Hong *, Xinghong Zhang, Jiancong Du, Wei Zhang

Center for Composite Materials and Structure, Harbin Institute of Technology, Harbin 150001, PR China

Received 5 May 2009; received in revised form 7 August 2009; accepted 18 August 2009
Available online 15 September 2009

Abstract

A camphene-based freeze-casting method was adopted to create ceramics with aligned, equiaxed pores applied so far exclusively for ceramics—is demonstrated for ZrO_2 porous ceramics. The pore volume fraction, channel size and pore shape were controlled by varying the freezing temperature, solid content and sintering condition. After sublimation of camphene, the samples were sintered for 2 h at elevated temperatures ranging from 1400 to 1550 °C. The initial level of solid loading played a primary role in the resulting porosity of the product. The porosity decreased from 82.5 to 65.5 vol.% when the solid loading was increased from 10 to 20 vol.%. The relationship of the compressive strength versus initial solid loading and sintering temperature was discussed. This technique is considered potentially useful in fabricating novel porous ceramics with special structure, and introduces a new application field of freeze-casting.

Keywords: Freeze-casting; Porosity; Mechanical properties; ZrO_2; Structural application

1. Introduction

High performance ceramics containing tailored porosity exhibit special properties and features that usually cannot be achieved by their conventional dense counterparts. The potentialities offered by highly porous ceramics are attracting considerably more attention today than just a few years ago.[1,2] Ceramics with low density (high porosity) can be engineered to combine several advantages inherent to their architecture, for example as supports for catalysts, artificial bones, ceramic filters, and light-weight parts used at high temperature.[2–4] To meet these requirements, various manufacturing methods are adopted to produce highly porous ceramics. These methods include the replication of polymer foams by ceramic dip coating, the foaming of aqueous ceramic powder suspensions, the pyrolysis of preceramic precursors, and the firing of ceramic powder compacts with pore-forming fugitive phases.[5–8]

Although the control over the structure and functional properties of cellular ceramics is continuously improving, all processing routes suffer from an inherent limitation: every processing route is intrinsically limited to a narrow range of pore characteristics. In addition, removal of the pore-forming agent can be a considerable problem.[7] An alternative method is to use the camphene-based freeze-casting route to fabricate porous ceramics. This has proven to be an attractive manufacturing approach as it allows construction of reticulated porous ceramics on a finer scale and without the polymer burnout stage during sintering.[9–12] Camphene can be frozen and easily sublimed near room temperature compared with other frozen vehicles (i.e., water[1,13] and tert-butyl alcohol[14]). This avoids some inherent problems currently associated with other manufacturing methods. It can produce interconnected pore channels in a tailored manner, e.g. aligned pore channels on a scale of several microns, which offers superior mechanical properties and functions. This method fundamentally makes full use of the three-dimensionally interconnected frozen vehicle network, which sublimes and in turn leaves pore channels in the ceramic body.[15–19] Moreover, it was found that the camphene-based freeze-casting method could be used to freeze very dilute ceramic slurries with low solid loadings, which, accordingly, allowed ultra-high porosity ceramics with completely interconnected pore channels to be produced.

The purpose of the present study was to explore the application of this method to the production of a highly porous ZrO_2 ceramics with aligned and interconnected porosity for

* Corresponding author. Tel.: +86 451 86403016; fax: +86 451 86403016.
E-mail address: hongcq@hit.edu.cn (C. Hong).

0955-2219/$ – see front matter © 2009 Elsevier Ltd. All rights reserved.
doi:10.1016/j.jeurceramsoc.2009.08.018

industrial engineering purposes and to determine the important variables that control the structural characteristics of the final product. The fabricated samples were characterized by evaluating the development of the pore structure and the mechanical properties.

2. Materials and methods

2.1. Materials selection

Commercially available yttria-stabilized zirconia doped with 5 mol%Y_2O_3 (0.4 μm, Fanmeiya powders Co. Ltd., Jiangxi, China) was used as the ceramic framework. Camphene ($C_{10}H_{16}$) (95% purity, Guangzhou Huangpu Chemical Factory, Guangzhou, China) was used as the freezing vehicle without any further purification. In addition, Texaphor 963 (Guangzhou Haichuan Co. Ltd., Guangzhou, China) was used as dispersant (density at 25 °C of 0.89–0.91 g cm^{-3}). The dispersant concentration was 3 wt.% of the ZrO_2 powder for all 10, 15 and 20 vol.% of solid loadings.

2.2. Solidification study

The solidification of the slurry was monitored by preparing an ZrO_2/camphene slurry at 60 °C with a solid loading of 10 vol.% and placing a drop into a pre-heated slide glass (about 60 °C for both top and bottom) in order to avoid rapid freezing. The size of drops for camphene-based slurry is about 4 mm in diameter. After dropping onto the prewarmed slide glass, it was then covered rapidly by another slide glass. Simultaneously the central position of the two slide glasses was covered by silicone rubber insulation. A detailed sketch is shown in Fig. 1. The drop was left to freeze at room temperature, after which the structure formed was examined using optical microscopy, with particular emphasis on observing the presence of primary and secondary dendrites.

2.3. Fabrication methods for bulk samples

The first part of the manufacturing process involved the slurry preparation. This was achieved by melting the camphene at a temperature of 60 °C on a heating plate to create a clear and fluid vehicle. The dispersant concentration was 5 wt.% of ZrO_2 powder for all solid loadings. The ZrO_2 powder was then added in quantities of 10, 15 and 20 vol.%.

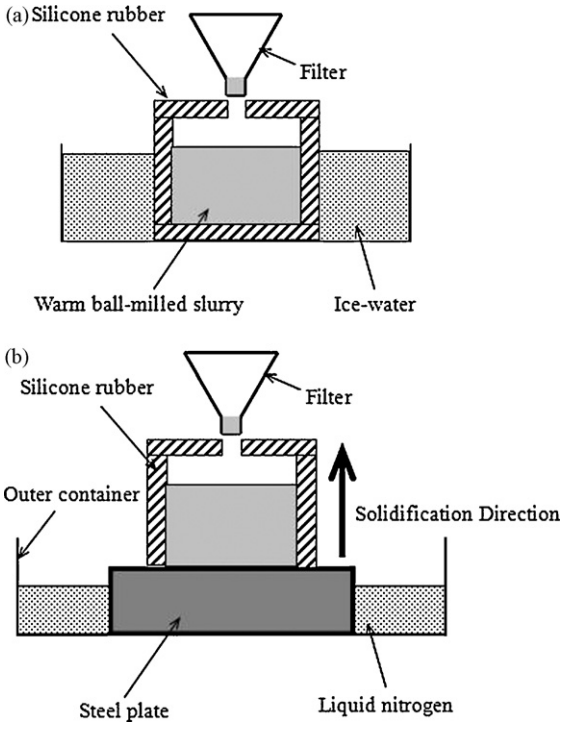

Fig. 2. A sketch of freezing assembly for fabricating cast body (a) in ice-water environment and (b) in liquid nitrogen cooling environment.

The slurry was stirred via the use of a motor and stirrer with a cap on the top to prevent any camphene vapour escaping. Zirconia/camphene/dispersant slurries with various zirconia contents (quantities of 10, 15 and 20 vol.%) were prepared by ball-milling at 60 °C for 20 h, before pouring into silicone rubber die for freezing; the moulds were 42 mm in internal diameter and 80 mm in height. The samples were left to cool at ice-water environment (0 °C) for 30 min. The detailed above sketch of the test setup is shown in Fig. 2(a). Meanwhile some samples were cooled at liquid nitrogen environment (−196 °C) for the same length of time to study the effect of cooling rate on the solidification characteristics, which can be seen from Fig. 2(b). After solidification, the green body was removed from the moulds and left to sublime (optimized to 24 h) at room temperature in order to remove the camphene entirely and achieve a highly porous

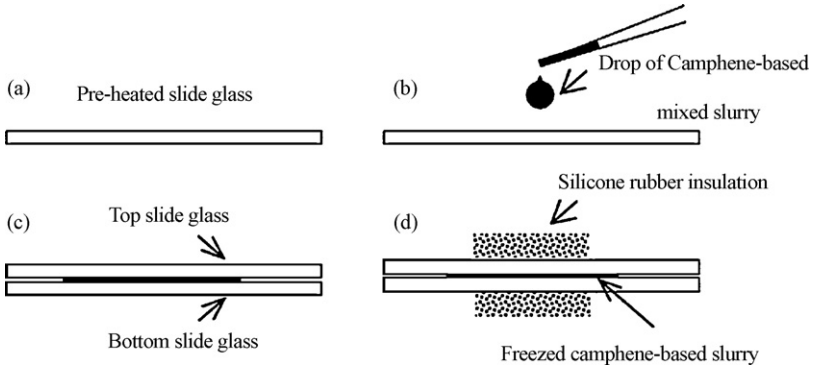

Fig. 1. A test sketch of freezing behavior for camphene-based slurry.

structure. Following sublimation, sintering of the green body at 1400–1550 °C enabled the densification of the samples and concomitant improvements in mechanical strength. The sintering regime entailed heating the samples at 0.5 °C/min up to 600 °C followed by 1 h of dwell time. They were then heated at 1 °C/min up to final sintering temperature and held at this temperature for 2 h, prior to cooling down to room temperature at the same rate of 20 °C/min.

2.4. Pore structure and compressive strength analysis

The fabricated samples were investigated by evaluating their pore structures, including pore size and porosity using scanning electron microscopy (SEM, Model S-4700, Japan). The porosity was calculated using mass and volume measurements to determine the density of the porous samples and then comparing this to that of the fully dense ceramic. Pore size was determined by measuring the average size of pores from the SEM micrographs taken at four points on each sample 3 mm from the outer wall (two samples per condition and four locations per sample).

For the compressive strength measurements, samples with a diameter of 6 mm and a height of 12 mm were loaded with a crosshead speed of 0.05 mm/min (Instron 3369, Instron Corp.). The present samples for mechanical tests were taken out from the central zone of the fabricated samples. The compressive loading and the orientation of the pores used for the pore size measurements are vertical and parallel to the solidification direction, respectively. The stress and strain responses were monitored; in excess of nine samples in each group of 10, 15 and 20 vol.% solid loadings were tested to obtain average values and standard deviations.

3. Results and discussion

3.1. Camphene solidification observations

The solidification phenomenon of the mixed slurry was investigated so as to acquire an understanding of the characteristics of pore and dendrite formation. Fig. 3(a) shows the development of long and straight dendritic branches near the marginal corner along the freezing plane, which runs towards the left corner (as shown by the arrow). Since the temperature gradient at the marginal region decreases fast, the camphene crystals grow dendritically in certain crystallographic directions. When the solidification was completed, a unique phase separated structure was produced, in which aligned camphene dendrites with a well-defined morphology surrounded by ZrO_2 particle networks were formed.

Fig. 3(b) shows the interconnectivity of the camphene branches near the central region of the slide where the temperature gradient was sufficiently high to stimulate secondary dendritic formation, and many short elongated camphene dendrites were formed randomly. A typical dendritic growth of camphene as well as ZrO_2 particle rejection of the warm slurry is shown in Fig. 4. It can be seen that the development of dendritic branches along the freezing plane, which, in the image, runs towards the top right corner. The particles are not only pushed

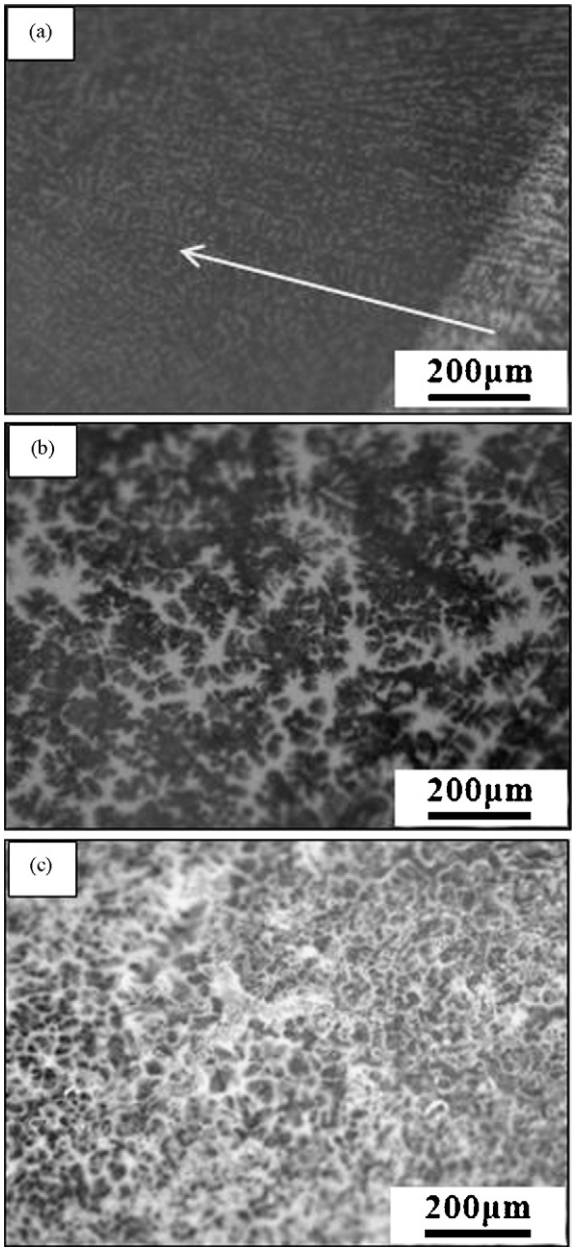

Fig. 3. Optical micrographs of the camphene dendritic growth during solidification (a) aligned camphene growth (shown by the arrow); (b) typical dendritic growth; (c) equiaxed camphene morphology.

along ahead of the advancing macroscopic solidification front composed of tips of growing dendrites, but are also connected on the spot after being rejected by dendrite arms.

The macro-morphology in the center region of the slide where no camphene dendrites were found (shown in Fig. 3(c)). Due to the low temperature gradient in the center region (since both top and bottom slide glass were covered by silicone rubber insulation), some of the dendrite side arms might be melted off and then act as seeds for new dendrites, resulting in the formation of equiaxed pore structures.[7] The above observations reveal the morphology of the dendrites that are produced during freezing of the camphene and the important role of the heat transfer gradient on determining the final shape and orientation.

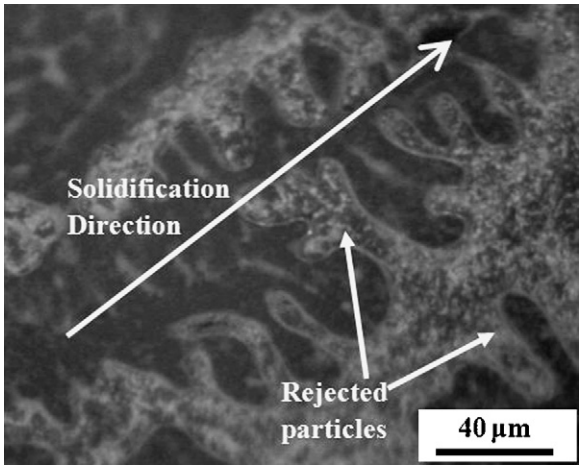

Fig. 4. Typical dendritic growth and particle rejection for camphene-based slurry.

3.2. Unidirectional solidification

Because the sintered pore structure form as replicas of camphene dendrites, unidirectional solidification was tried to control the growth direction of the camphene dendrites. A special mold composed of a steel bottom plate and a silicone rubber die on it was prepared to create a cylindrical cavity. Warm ball-milled ZrO_2 slurry of 60 °C with 15 vol.% solid content was poured at room temperature into the prewarmed mold having almost the same temperature as the slurry. Just after casting, liquid nitrogen was poured into the outer container to cool only the steel bottom plate so that the solidification of the camphene-based slurry would occur unidirectionally from the bottom towards the top in the mold. The solidification was completed in about 3 min, and then the cast body was dried in an ambient atmosphere for 30 h.

Sintered samples generated with solid loadings of 15 vol.% were analyzed by SEM. The SEM micrographs (Fig. 5(a) and (b)) showed that the pores tend to align in the direction of freezing, indicating the possibility of controlling pore orientation by controlling parameters such as the heat transfer gradient and direction of freezing. Since the chilled mold was suddenly cooled with liquid nitrogen about −160 °C, the camphene rapidly cooled below its solidification temperature, and thus many nuclei of the camphene then form on the mold wall and begin to grow into the warm slurry. Under these conditions, most of the nuclei do not have a preferential orientation that corresponds to the direction of the heat conduction. Therefore, these camphene crystals cannot overgrow dendritically, and this results in the formation of long straight channels in the sintered body (see Fig. 5).

Beyond the above region, the temperature gradient near the die wall decreases and the camphene crystals began to grow dendritically in certain crystallographic directions. Those crystals with a preferential orientation close to the direction of heat flow, i.e., parallel to the mold wall, grow faster and can lead to their secondary dendritic formation. It is accordingly results in the elongated aligned pore channels and short arms channel in the sintered body, as shown in Fig. 5(c).

In the center of the cast body, some of the dendrite side arms might be melted off and then act as seeds for new dendrites, resulting in the formation of equiaxed pore structures (shown in Fig. 5(d)). This unique pore structure in the center of the cast body might be related to the breakaway of the side arms from the primary dendrite of the camphene.

3.3. Effect of solid content on sintered materials

Solid loading plays an important role in determining the porosity and mechanical strength characteristics of the sintered samples. Fig. 6(a)–(c) shows the pore structures after sintering at 1500 °C with the solid loading varying from 10 to 20 vol.%. It is clear that lower solid loading results in higher porosity and larger pore sizes, while the sintered zirconia walls became thinner. During freezing, the camphene dendrites can grow until the force created by the particle concentration exceeds the capillary drag force pushing the particles with the solid/liquid interface.[19,20] Therefore, it is reasonable to suppose that a lower solid loading will lead to the formation of larger camphene dendrites and thinner concentrated ZrO_2 ceramic walls.

Fig. 7 shows the relationship between the porosity and the initial solid loading of the ceramic slurry. As the solid loading is increased, the porosity was found to decrease proportionately. The porosity was reduced from 81.5 to 65.5% by increasing the solid loading from 10 to 20 vol.%. The linear relationship between the porosity and the initial solid content can be expressed as follows:

$$P = 97.5 - 1.6x \quad (1)$$

where P is the porosity (vol.%) and x is the solid loading (vol.%).

This result suggests that the porosity can be manipulated by empirically controlling the initial solid loading used in the ceramic/camphene slurry. It should be noted that the possible sublimation of the molten camphene during ball-milling the freeze-casting is not considered in the above equation. From these observations, it is obvious that the camphene-based freeze-casting is very useful for producing high porous ceramics with porosities and completely interconnected pore channels, as well as well sintered ZrO_2 walls.

The main physical and mechanical properties of the sintered samples are summarized in Table 1. The results show that after being sintered with a lower solid content, the sample acquired from 10 vol.% slurry was so light that bulk densities were even lower than water (1 g/cm^3). As the initial solid loading was increased, the compression strength increased from 16.2 to 53.4 MPa. Fig. 8 shows the stress–strain curves for 10, 15 and 20 vol.% ZrO_2 solid content sintered at 1500 °C. All curves shown almost elastic deformation followed by a transition or plateau stage. No sudden drops or catastrophic fracture are observed, although load drops are found after showing a peak load.

Generally, the strength of a porous ceramic is strongly affected not only by the porosity, but also by the formation of sintering neck on the ceramic wall as well as the smaller pore size (several tens of microns) compared conventional processing

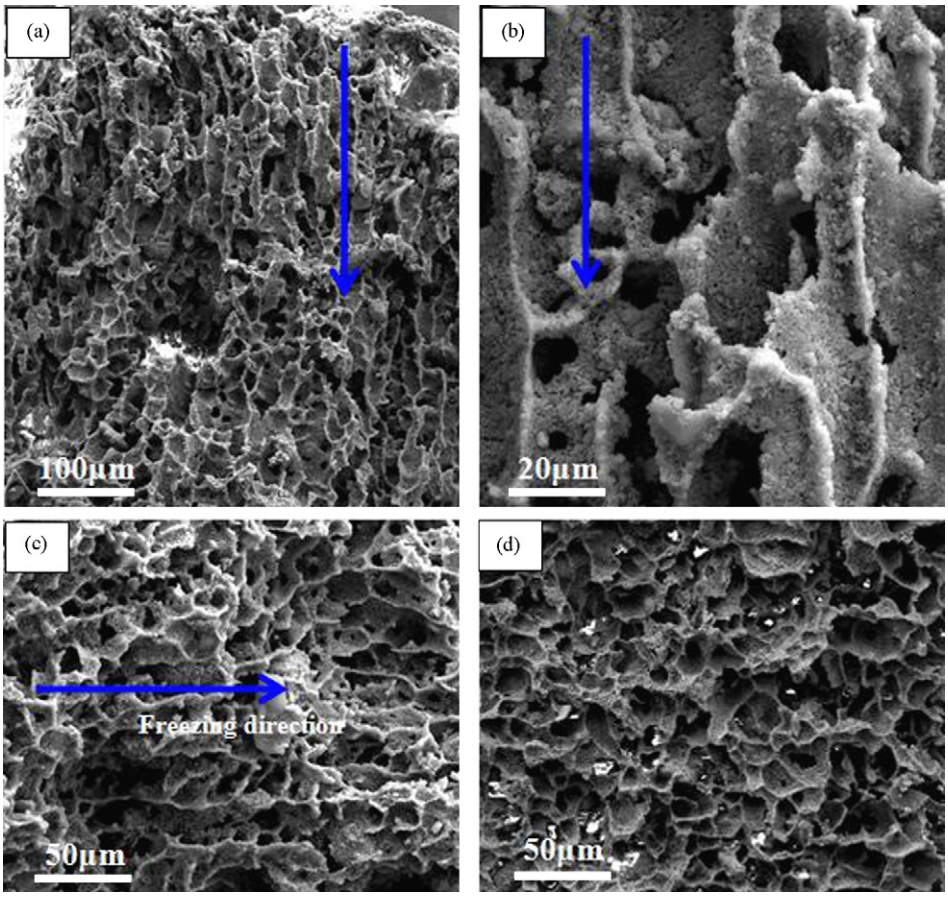

Fig. 5. (a) Pore alignment in the direction of freezing; (b) magnified microstructure in Fig. 2(a); (c) dendritic pore distribution beyond the die wall; (d) equiaxed pore morphology in the center of sintered sample.

methods (>100 μm). In this observation, pore size was determined by measuring the average size of pores from the SEM micrographs taken at several points on the polished surface. For example, for the 10 and 15 vol.% ZrO_2 solid content sintered at 1500 °C, the pore sizes of the prepared sampled approximately ranged from 15 to 30 μm (Fig. 9(a) and (b)). Furthermore remarkable sintering necks were formed (shown in Fig. 6(d)), resulting in high mechanical properties.

3.4. Effect of sintering temperature on structure

The evolution of microstructure sintered at elevated temperatures ranging from 1400 to 1550 °C is shown in Fig. 10(a)–(d). It can be concluded that with a given initial solid loading (15 vol.%), the sintering temperature significantly contributes to the change of ceramic struts and porosity. As the sintering temperature is increased, the ZrO_2 ceramic struts are greatly densified (i.e., loosely bonded particles are observed from Fig. 10(a), while the sintering struts are greatly enhanced in view of Fig. 10(d)). The effect of sintering temperature on the porosity was also investigated, and the results are shown in Fig. 11.

The experimental examinations (as shown in Fig. 11) revealed that the porosity decreases and compressive strength goes up when sintering temperature increases from 1400 to 1550 °C (i.e., 18–59 MPa for compressive strength). Both then reach a comparable plateau value, which means that densification is achieved at 1500 or 1550 °C. Further increase in sintering temperature will deteriorate the pore structure. Therefore, the optimum sintering temperature was determined to be 1500 °C in this work. Here, it is worth noting the increasing of ZrO_2 grain size with temperature variation is very limited from the experimental observation (see Fig. 10(a)–(d)). Although the proper reasons of this particular phenomenon are still to be explored, it is probably partly

Table 1
Properties of ZrO_2 with different initial densities after sintered at 1500 °C for 2 h.

Slurry solid loading (vol.%)	Bulk density after sintering (g/cm^3)	Compression strength (MPa)	Porosity content
10	0.93–0.96	16.2	81.5%
15	1.20–1.29	32.9	74.4%
20	1.68–1.75	53.4	65.5%

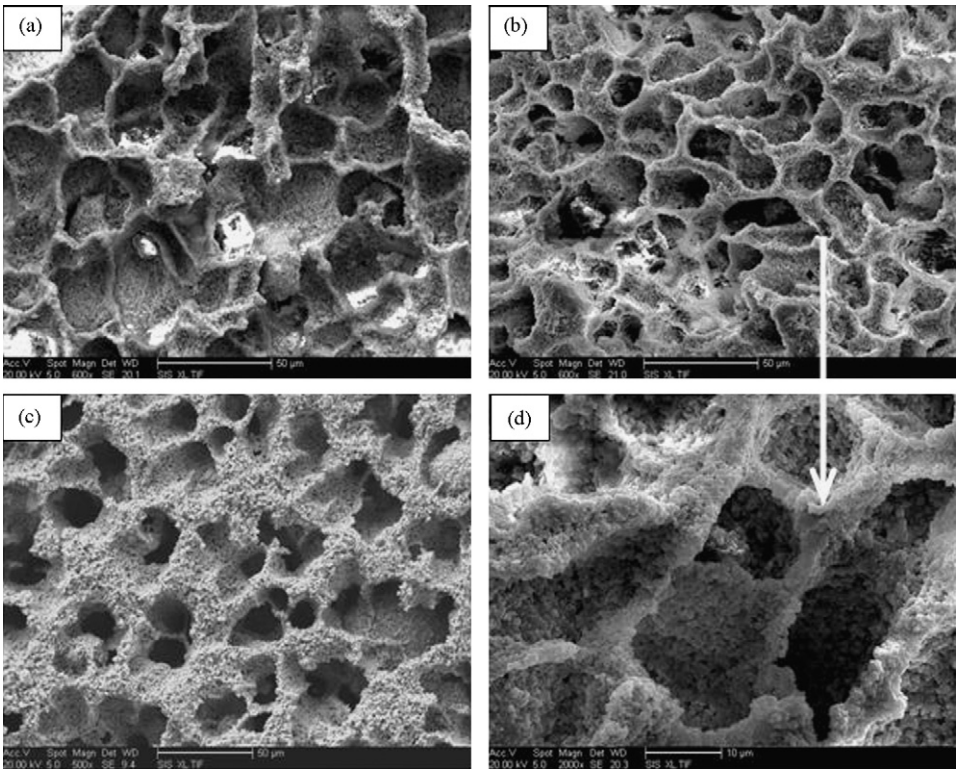

Fig. 6. SEM micrographs of porous structures sintered at 1450 °C for (a) 10 vol.%, (b) 15 vol.%, (c) 20 vol.%, and (d) sintered ceramic wall in solid loading of 15 vol.%.

related to the pinning of grain boundary at the surface during sintering of thin films, when the grain size lies in the same range of order as the lamellate thickness.

Highly porous ceramics fabricated by conventional methods often contain defects, such as cracking and surface flaws. For example, reticulated porous ceramics produced using the polymer replication method have longitudinal cracks and surface flaws on the sintered ceramics struts during pyrolysis of the polymeric sponge. Cellular structures prepared by direct foaming usually exhibit mechanical strengths higher than that of replica techniques due mainly to the absence of flaws in the cell struts, the sintered foams show moderate compressive strengths of up to 16 MPa in alumina foams with porosities of 88% produced from particle-stabilized foams.[21,22] Using camphene as the solvent, dilute ZrO_2 slurries were produced and large shrinkage during drying was avoided. By adjusting the initial solid loading and sintering temperatures, light-weight ZrO_2 ceramics with controlled microstructures and properties were prepared. It was possible to increase the porosity from 65.5 to 84.5%, while still obtaining high mechanical strength (over 16 MPa). In addition, the prepared samples produced using camphene as solvent showed well-constructed zirconia walls without any noticeable defects, which might enable them to have good mechanical properties.

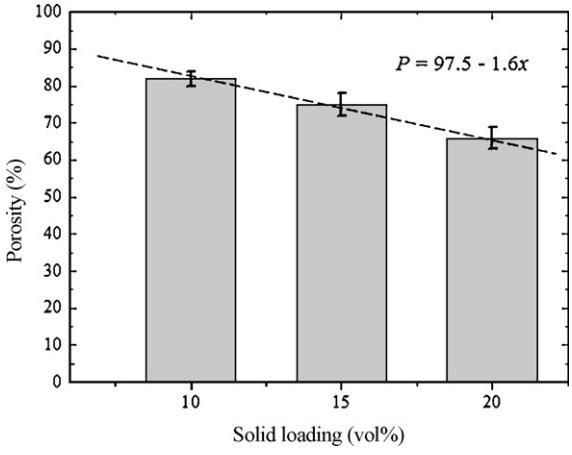

Fig. 7. Measured porosity (P) of the porous ZrO_2 ceramics sintered at 1500 °C for 2 h as a function of the initial solid loading.

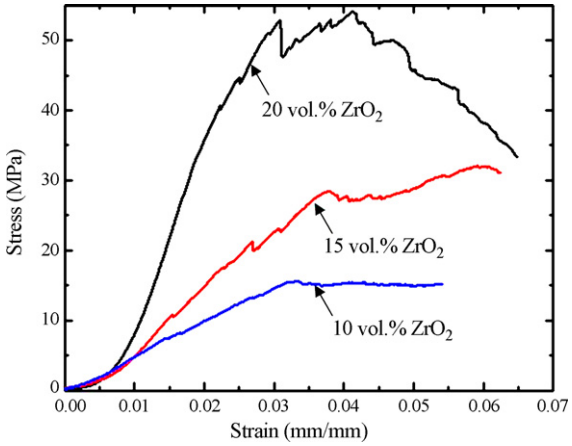

Fig. 8. The stress–strain curves for 10, 15 and 20 vol.% ZrO_2 solid content sintered at 1500 °C.

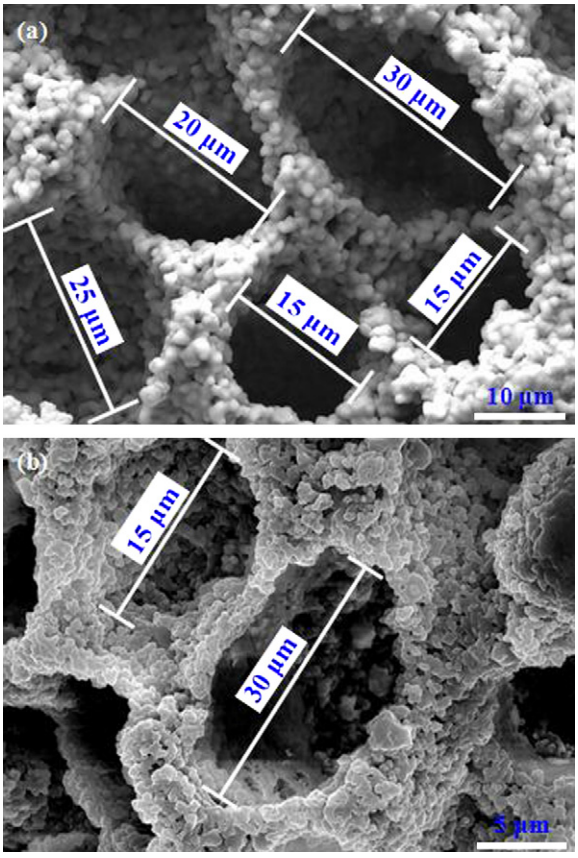

Fig. 9. Pore size calculated from polished surface (a) 10 vol.% and (b) 15 vol.% ZrO_2 solid content sintered at 1500 °C.

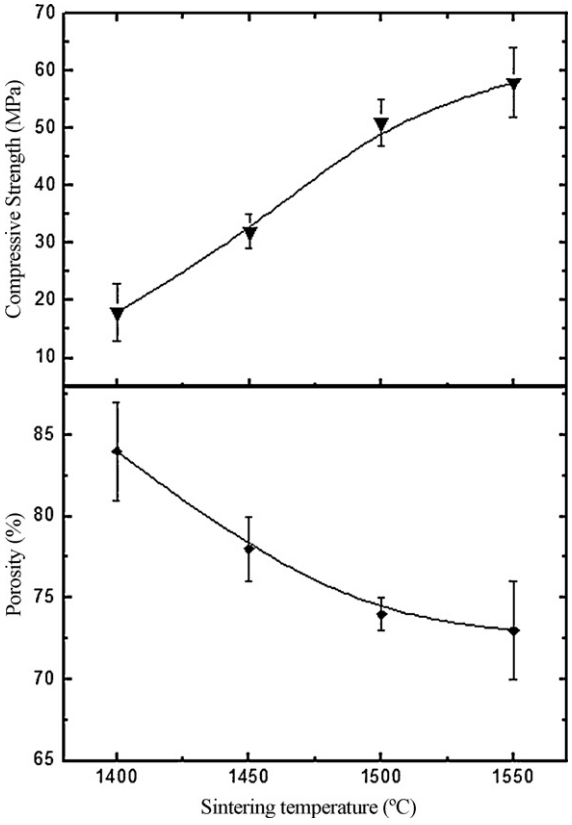

Fig. 11. Influence of sintering temperature (2 h at dwell temperature) on compressive strength and total porosity.

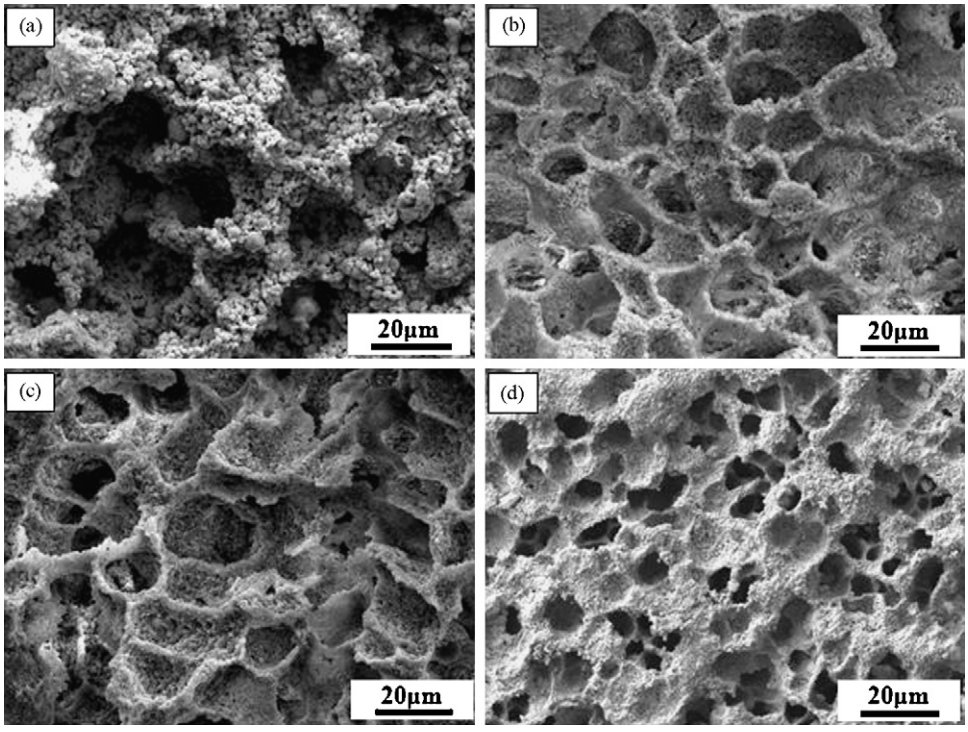

Fig. 10. Scanning electron micrographs of the samples sintered for 2 h in air at (a) 1400 °C, (b) 1450 °C, (c) 1500 °C and (d) 1550 °C in solid loading of 15 vol.%.

4. Conclusions

This paper demonstrated that special pore shape and size can be achieved using the novel fabricating technique of freeze-casting, indicative of the potential for highly porous ZrO_2 samples to be produced using this method.

Initial solid loading played an important role in the resulting porosity of the materials. This was reduced from 81.5 to 65.5% by increasing the solid loading from 10 to 20 vol.%. As a result of this, the compressive strength was affected, increasing from 16.2 to 53.4 MPa for the respective increase in solid loading. The rate of heat transfer affected the final morphology of the dendrites; camphene dendrites were found to orient according to the direction of freezing under liquid nitrogen environment; the sintering temperature (from 1400 to 1550 °C) also affected the porosity and mechanical properties. The porosity (for 15 vol.% solid content) ranged from 73.5 to 84.5 vol.%, while the compressive strength increased from 18 to 59 MPa, respectively.

In conclusion, this manufacturing technique shows great potential for generating defect-free porous ceramics with controlled porosity and pore size and appropriate compressive properties for use in modern engineering applications.

Acknowledgements

Authors acknowledge the support of the National Natural Science Funds for Distinguished Young Scholar (No. 10725207) and the Foundation for Innovative Research Groups of the National Natural Science Foundation of China (No. 10821201) and the National Natural Science Foundation of China (No. 50702016). We show thanks to the support of Doctoral Program of Higher Education of Ministry of Education of China (No. 200802131047) and the first special grant of China Postdoctoral Science Foundation (No. 200801286).

References

1. Deville, S., Freeze-casting of porous ceramics: a review of current achievements and issues. *Adv. Eng. Mater.*, 2008, **10**, 155–169.
2. Deville, S., Saiz, E. and Tomsia, A. P., Freeze casting of hydroxyapatite scaffolds for bone tissue engineering. *Biomaterials*, 2006, **27**, 5480–5489.
3. Gough, J. E., Clupper, D. C. and Hench, L. L., Osteoblast responses to tape-cast and sintered bioactive glass ceramics. *J. Biomed. Mater. Res.*, 2004, **69**, 621–628.
4. Yuan, H. P., Bruijn, J. D., Zhang, X. D., Blitterswijk, C. A. and Groot, K., Bone induction by porous glass ceramic made from bioglass (R) (45S5). *J. Biomed. Mater. Res.*, 2001, **58**, 270–276.
5. Clupper, D. C., Mecholsky, J. J., LaTorre, G. P. and Greenspan, D. C., Bioactivity of tape cast and sintered bioactive glass–ceramic in simulated body fluid. *Biomaterials*, 2002, **23**, 2599–2606.
6. Boaro, M., Vohs, J. M. and Gorte, R. J., Synthesis of highly porous yttria-stabilized zirconia by tape-casting methods. *J. Am. Ceram. Soc.*, 2003, **86**, 395–400.
7. Koh, Y. H., Lee, E. J., Yoon, B. H., Song, J. H. and Kim, H. E., Effect of polystyrene addition on freeze casting of ceramic/camphene slurry for ultra-high porosity ceramics with aligned pore channels. *J. Am. Ceram. Soc.*, 2006, **89**, 3646–3653.
8. Schmidt, H., Koch, D. and Grathwohl, G., Micro-/macroporous ceramics from preceramic precursors. *J. Am. Ceram. Soc.*, 2001, **84**, 2252–2255.
9. Lee, E. J., Koh, Y. H., Yoon, B. H., Kim, H. E. and Kim, H. W., Highly porous hydroxyapatite bioceramics with interconnected pore channels using camphene-based freeze casting. *Mater. Lett.*, 2007, **61**, 2270–2273.
10. Yook, S.-W., Kim, H.-E. and Koh, Y.-H., Fabrication of porous titanium scaffolds with high compressive strength using camphene-based freeze casting. *Mater. Lett.*, 2009, **63**, 1502–1504.
11. Macchetta, A., Turner, I. G. and Bowen, C. R., Fabrication of HA/TCP scaffolds with a graded and porous structure using a camphene-based freeze-casting method. *Acta Biomater.*, 2009, **5**, 1319–1327.
12. Kiyoshi, A. and John, W. H., New freeze-casting technique for ceramics with sublimable vehicles. *J. Am. Ceram. Soc.*, 2004, **87**, 1859–1863.
13. Deville, S., Saiz, E., Nalla, R. K. and Tomsia, A., Freezing as a path to build complex composites. *Science*, 2006, **311**, 515–518.
14. Chen, R. F., Huang, Y., Wang, C. A. and Qi, J. Q., Ceramics with ultra-low density fabricated by gelcasting: an unconventional view. *J. Am. Ceram. Soc.*, 2007, **90**, 3424–3429.
15. Koh, Y. H., Sun, J. J. and Kim, H. E., Freeze casting of porous Ni-YSZ cermets. *Mater. Lett.*, 2007, **61**, 1283–1287.
16. Jun, I. K., Koh, Y. H., Song, J. H., Lee, S. H. and Kim, H. E., Improved compressive strength of reticulated porous zirconia using carbon coated polymeric sponge as novel template. *Mater. Lett.*, 2006, **60**, 2507–2510.
17. Yoon, B. H., Choi, W. Y., Kim, H. E., Kim, J. H. and Koh, Y. H., Aligned porous alumina ceramics with high compressive strengths for bone tissue engineering. *Scripta Mater.*, 2008, **58**, 537–540.
18. Waschkies, T., Oberacker, R. and Hoffmann, M. J., Control of lamellae spacing during freeze casting of ceramics using double-side cooling as a novel processing route. *J. Am. Ceram. Soc.*, 2009, **92**, S79–S84.
19. Araki, K. and Halloran, J. W., Porous ceramic bodies with interconnected pore channels by a novel freeze casting technique. *J. Am. Ceram. Soc.*, 2005, **88**, 1108–1114.
20. Cadirli, E., Marasli, N., Bayender, B. and Gunduz, M., Dependency of the microstructure parameters on the solidification parameters for camphene. *Mater. Res. Bull.*, 2000, **35**, 985–995.
21. Gonzenbach, U. T., Studart, A. R., Tervoort, E. and Gauckler, L. J., Macroporous cermics from particle-stabilized wet foams. *J. Am. Ceram. Soc.*, 2006, **90**, 16–22.
22. Studart, A. R., Gonzenbach, U. T., Tervoort, E. and Gauckler, L. J., Processing routes to macroporous ceramics: a review. *J. Am. Ceram. Soc.*, 2006, **89**, 1771–1789.